Free evolution in the Ginzburg-Landau equation and other complex diffusion equations

Southgate, Howard N.

DOI
10.1088/1402-4896/ad8aa0

Publication date
2024

Document Version
Final published version

Published in
Physica Scripta

PAPER • **OPEN ACCESS**

Free evolution in the Ginzburg-Landau equation and other complex diffusion equations

To cite this article: Howard N Southgate 2025 *Phys. Scr.* **100** 015261

Physica Scripta

PAPER

Free evolution in the Ginzburg-Landau equation and other complex diffusion equations

Howard N Southgate

Faculty of Civil Engineering and Geosciences, Delft University of Technology, The Netherlands

E-mail: h.n.southgate@tudelft.nl

Keywords: complex diffusion, free evolution, nonlinear waves, Ginzburg-Landau equation, Schrödinger equation, channel bars

OPEN ACCESS

RECEIVED
31 July 2024

REVISED
12 October 2024

ACCEPTED FOR PUBLICATION
23 October 2024

PUBLISHED
20 December 2024

Abstract

New ordinary differential equations (ODEs) for the evolution of spectral components are derived from the complex Ginzburg–Landau equation (CGLe) for one-dimensional spatial domains without boundaries (free evolution) and with one fixed boundary (semi-free evolution). For such evolution, a complex or imaginary diffusion term creates a tendency for waves to lengthen. This requires a novel ansatz and auxiliary condition that treat wavenumbers as time-varying. The ansatz consists of a discrete spatial Fourier transform modified with a time-dependent wavenumber for the peak spectral component. The wavenumbers of the other components are fixed relative to this wavenumber. The new auxiliary condition is the terminal condition for complex diffusion (after wavenumbers evolve to zero, they remain at zero). The derived free and semi-free ODEs are solved along characteristic lines located symmetrically about a fixed spatial point. Waves lengthen with time away from this point in both directions. Laboratory experiments on the formation of channel sandbars, theoretically described by the CGLe, show two regions whose evolutionary behaviour is qualitatively predicted by the free and semi-free evolution equations. This analysis applies to other time-dependent partial differential equations with complex or imaginary diffusion terms. New freely evolving solutions are derived for the complex heat equation and Schrödinger equation (linear and nonlinear).

1. Introduction

Several partial differential equations (PDEs) with physical applications contain a complex diffusion term of the form $(\alpha_r + i\alpha_i)\partial^2\Psi/\partial X^2$, where α_r and α_i are real constants, $i = \sqrt{-1}$, $\Psi(X,\ T)$ is the complex amplitude of a system variable, X is distance and T is time. These PDEs can be derived for a particular time and space scale from a multiple-scale analysis of the (real) physical system equations. The imaginary part of the complex diffusion term implies that solutions of these PDEs have wavelike as well as diffusive properties. Two examples with many applications in physics are the complex Ginzburg–Landau equation (CGLe) and nonlinear Schrödinger equation (NLSe) [1–17].

An aim of this study is to derive particular solutions of these complex diffusion equations for free evolution (i.e. without spatial boundaries or other external constraints) in one-dimensional spatial domains. For many applications, the auxiliary conditions for particular solutions are provided by initial and boundary conditions. In experiments with bounded spatial domains, the boundaries often have an important role in pattern creation and stability, which theories attempt to predict using boundary conditions appropriate to the experiments [9, 10]. Many mathematical and numerical studies use periodic boundary conditions [1, 10–12], which maintain Galilean invariance and thereby reduce the number of equation constants. However, periodic boundary conditions cannot represent free evolution. For a finite spatial domain, they restrict or select wavenumbers in space-periodic solutions. In the limit as the domain length tends to infinity, they constrain the wavenumbers in these solutions to be time-constant. The application to free evolution requires auxiliary conditions that are different from any spatial boundary condition.

An innovation in this study is to obtain the auxiliary conditions for free evolution from the terminal (i.e. final or end-time) condition for a complex diffusive process, as well as from the initial condition. Complex diffusion describes a physical process in which waves can lengthen with time. The terminal condition states that after a wavenumber, $k(T)$, has evolved to zero, no further evolution of k takes place, i.e. $dk/dT = 0$ when $k = 0$. One implication of the terminal condition is that it disallows antidiffusive solutions in which waves shorten with time. This satisfies the well-posedness requirement for continuous dependence on initial data. The full role of the terminal condition in deriving the particular solution for free evolution is described in section 3.2.1.

Another novelty is the ansatz from which the particular solution for free evolution is derived. This ansatz consists of a discrete spatial Fourier transform modified to have wavenumbers as continuous functions of time. The particular solution for free evolution is derived in the form of characteristic lines along which the amplitudes, wavenumbers and phases of spectral components evolve as functions of time only. Coupled, first-order, ordinary differential equations (ODEs) are derived for the evolution of these parameters. The particular solution has a fixed spatial point with reflection symmetry. Waves lengthen with time away from this point in both directions. The location of the fixed point may be determined by perturbations in the initial condition.

In physical applications, the spatial domain is necessarily finite, but free evolution can occur if the domain is sufficiently long that the boundaries only influence shorter regions adjacent to them. The particular solution for free evolution applies in the interior of the domain away from these boundary regions. Free evolution is contrasted with 'bounded' evolution, which occurs in spatial domains that are sufficiently short that the influence of the boundaries extends throughout the domain [1, 6–8]. For bounded evolution, the wavenumbers in space-periodic solutions are constrained by the boundary conditions to be time-constant. The type of evolution (free or bounded) in a given domain length can depend on the material medium properties (section 6). A video comparing free and bounded spectral evolution is shown in appendix C.

This work also considers 'semi-free' evolution in which the spatial domain has a single fixed boundary but is otherwise unrestricted. The derivation of the particular solution for semi-free evolution is similar to that for free evolution, but the auxiliary conditions are obtained from the condition at the single boundary as well as from the terminal and initial conditions. Semi-free evolution can occur in a boundary region of a long domain, with a short transition to the region of free evolution in the interior of the domain. Experimental examples of free and semi-free evolution for space-periodic channel sandbars, theoretically described by the CGLe [17], are shown in section 4. Several such experiments show that these bars lengthen as they grow in amplitude [18–22].

This study concerns space-periodic solutions without local defects, but modified with time-dependent wavenumbers. The focus is on nonlinear PDEs whose solutions evolve to sideband-stable SFP (stationary, finite-amplitude, plane-wave) states, as well as on linear PDEs. Some implications for nonlinear PDEs with sideband-unstable SFP states are briefly discussed in section 6. The particular solution for free evolution is derived initially for the CGLe (section 3). The equivalent solutions for other PDEs with complex or imaginary diffusion terms are then obtained as special cases by setting some of the constants in the CGLe to zero (section 5). For these cases, some straightforward modifications to the ansatz are required to treat nonlinear terms and the differences in scaling and initial conditions.

The remainder of the paper is structured as follows. Section 2 describes some of the main properties of the CGLe required for the new work. Section 3.1 derives the general evolution equations from the CGLe for the new ansatz. Section 3.2 derives the particular equations for free evolution, using the terminal condition for complex diffusion. Section 3.3 adapts these equations for semi-free evolution. Section 4 presents qualitative evidence for the free and semi-free evolution equations from laboratory experiments on channel sandbars. Section 5 derives free evolution equations for other time-dependent PDEs containing a complex or imaginary diffusion term, as special cases of the CGLe. Section 6 discusses some ideas for future studies. Section 7 summarises the main conclusions. Appendix A considers the normalisation of the evolution equations and derives a simplification by including only coherent nonlinear terms. Appendix B demonstrates the Galilean invariance of free solutions of the CGLe. Appendix C shows a video of the evolution of wave spectra for free and bounded solutions.

2. Background to the CGLe

2.1. The CGLe and scaling

In partially scaled time (T) and space (X) coordinates the CGLe is

$$\frac{\partial \Psi}{\partial T} = (\gamma_r + i\gamma_i)\Psi + (\alpha_r + i\alpha_i)\frac{\partial^2 \Psi}{\partial X^2} - (\mu_r - i\mu_i)|\Psi|^2\Psi \tag{2.1}$$

where Ψ is the partially scaled complex amplitude and γ_r, γ_i, α_r, α_i, μ_r and μ_i are real constants (referred to as the 'CGLe constants') derived from normalised variables in the underlying physical equations, with $\gamma_r \geqslant 0$ and $\alpha_r \geqslant 0$. Ψ describes the modulation of a plane base wave. The partially scaled variables Ψ, X and T are related to the unscaled variables with subscript u by

$$\Psi = \Psi_u/\varepsilon \qquad X = \varepsilon X_u \qquad T = \varepsilon^2 T_u \tag{2.2}$$

The scaling factor, ε ($0 < \varepsilon < 1$), is defined by $\varepsilon^2 = (R - R_c)/R_c$ where R is a system constant whose value moderately exceeds a critical value, R_c, at which a spatially uniform state is marginally unstable. A fully scaled form of the CGLe is

$$\frac{\partial \Psi_f}{\partial T_f} = \Psi_f + (1 + ic_1)\frac{\partial^2 \Psi_f}{\partial X_f^2} - (1 - ic_2)|\Psi_f|^2\Psi_f$$
$$c_1 = \alpha_i/\alpha_r \qquad c_2 = \mu_i/\mu_r \tag{2.3}$$

The scaling relations for Ψ_f, X_f and T_f are functions of the CGLe constants [1, 4]. The fully scaled CGLe (2.3) is used in section 2.4 for comparison with previous studies, but the rest of the paper uses the partially scaled CGLe (2.1) in order that variables are closer to quantities measured in experiments and to consider cases where some of the CGLe constants are zero.

General values of wavenumber and frequency are denoted by k, ω, the base wave values by k_r, ω_r and their differences by K, Ω

$$K = k - k_r \qquad \Omega = \omega - \omega_r \tag{2.4}$$

The wavenumbers are scaled by ε^{-1} and frequencies by ε^{-2}, giving $kX = k_u X_u$, $\omega T = \omega_u T_u$, $KX = K_u X_u$ and $\Omega T = \Omega_u T_u$. The CGLe can express information on K and Ω but not k_r or ω_r. Accordingly, K and Ω are called the 'wavenumber' and 'frequency' in analyses of the CGLe and NLSe (sections 2.2–2.4, 3, 5.3 and the appendices). The parameters k and ω are termed the 'total' wavenumber and frequency; 'total' refers to the modulation combined with the base wave. The auxiliary conditions may incorporate k_r or ω_r.

2.2. Initial and terminal conditions

Solving the CGLe is treated as an initial value problem in which Ψ is set at an initial time, $T = 0$, and remains bounded in amplitude at all future times. The initial condition is usually a spatially uniform state, $\Psi = 0$. This state is unstable to perturbations in a limited wavenumber range of width $O(\varepsilon)$ in unscaled units, centred on $K = 0$. This central wavenumber component has the fastest growing amplitude initially.

The complex diffusion term tends to homogenise spatial gradients in Ψ by reducing both the amplitudes and wavenumbers of the spectral components. For bounded evolution, the boundary conditions constrain wavenumbers to be time-constant, but for free and semi-free evolution, wavenumbers can evolve to smaller values. In the latter cases, the terminal condition for complex diffusion (postulated in this study as an auxiliary condition) yields an ODE for wavenumber evolution (section 3.2). This terminal state might not be reached because of other non-diffusive processes but there is a diffusive tendency towards this state.

2.3. Plane-wave solutions

SFP solutions of the CGLe are derived from the ansatz

$$\Psi = A \exp\left[i(K(X - X_0) - \Omega T)\right] \tag{2.5}$$

where A is the absolute amplitude, K and Ω are given by (2.4), and X_0 is a reference location. Substituting (2.5) in (2.1) yields

$$\alpha_r K^2 = \gamma_r - \mu_r A^2 \tag{2.6}$$

$$\alpha_r \Omega = \alpha_i \gamma_r - \alpha_r \gamma_i - (\alpha_i \mu_r + \alpha_r \mu_i)A^2 \tag{2.7}$$

Equations (2.6) and (2.7) represent a family of SFP solutions of the CGLe in which K and Ω are functions of the amplitude, A. These solutions are unstable to sideband perturbations for certain ranges of values of the CGLe constants [5].

A non-stationary, plane-wave solution of the CGLe is derived if A and Ω are time-dependent in (2.5) and the wavenumber is constrained as a constant, K_a. This ansatz yields decoupled equations for dA/dT and $d\Omega/dT$, with analytical solutions for $A(T)$ and $\Omega(T)$. These solutions in the limit, $T \to \infty$, are known as the 'Stokes wave' and are equivalent to setting $K = K_a$ in (2.6) and (2.7).

2.4. Bounded evolution equations for the CGLe

Space-periodic evolution equations for a finite spatial domain can be derived from the CGLe using a discrete spatial Fourier transform [6–8]

$$\Psi_f(X_f, T_f) = \sum_{n=-N}^{N} Z_n(T_f) \exp\left[inq(X_f - X_{f0})\right] \tag{2.8}$$

In (2.8), q is the width of the spectral components (i.e. their wavenumbers are $K_n = nq$), X_{f0} is a reference location, Z_n are complex variables, and N is a truncation limit for numerical computations. Following [6],

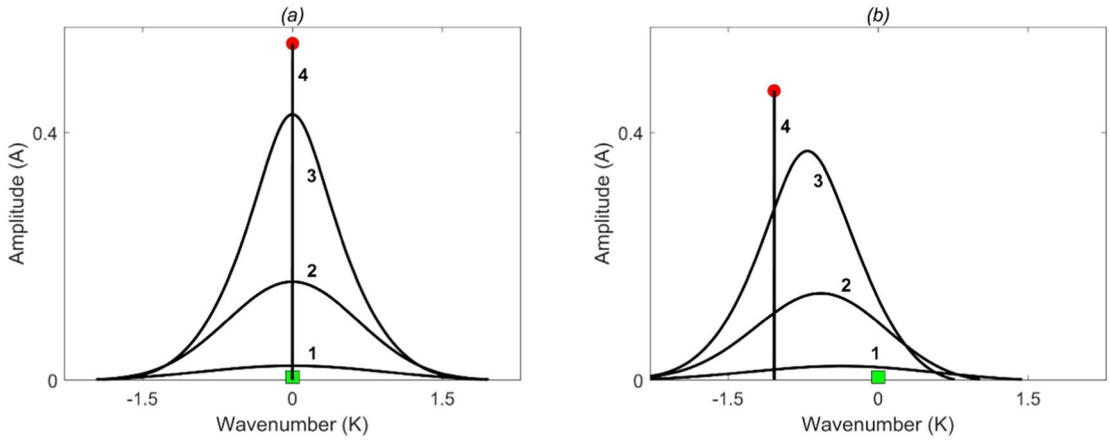

Figure 1. Evolution of wave spectra in the CGLe. (a, left) Bounded evolution with time-constant wavenumber components [6–8]. (b, right) Free evolution to smaller wavenumbers (this study). Green square: starting position of the central wavenumber component. Red circle: sideband-stable final state. Higher numbers denote spectra at later times. Both figures start with the same low-amplitude spectrum spanning the unstable wavenumber range in a perturbed $\Psi = 0$ state. See the figure 2 caption for further details. A video showing both types of evolution is provided in appendix C.

substitution of (2.8) in the fully scaled CGLe (2.3) yields a set of $N + 1$ complex equations

$$dZ_n/dT_f = (1 - n^2q^2(1 + ic_1))Z_n - (1 - ic_2) \sum_{\substack{j+l+m=n \\ |j|,|l|,|m| \leqslant N}} Z_j Z_l Z_m^* \tag{2.9}$$

where * denotes the complex conjugate, $n = 0, 1, \ldots, N$ and $Z_{-n} = Z_n$. Neumann conditions are applied at the boundaries. Numerical simulations of (2.9) for $1 - c_1c_2 > 0$ have shown that solutions evolve towards a sideband-stable SFP state with $n = 0$ (the Stokes wave). This was demonstrated both for large values of N [7] and for strong truncation ($N = 1, 2, 3$) [6]. These studies also investigated cases for $1 - c_1c_2 < 0$, for which SFP states are sideband-unstable and complex dynamics can occur.

The present study considers cases with $1 - c_1c_2 > 0$ which should, according to (2.9), evolve towards the Stokes wave. However, such evolution contradicts several laboratory experiments that show wavelengths increasing with time (section 4). The boundary conditions for (2.9) are assumed to have an influence that extends throughout the spatial domain, resulting in bounded evolution. The observed evolution in the experiments is believed to be free and semi-free evolution, for which novel solutions are derived in section 3. Figure 1 and the video compare free and bounded spectral evolution using the same CGLe constants and initial condition.

3. Free and semi-free evolution equations for the CGLe

Novel particular solutions of the CGLe for free and semi-free evolution are derived in this section. In section 3.1, general evolutionary ODEs are derived from an ansatz consisting of a discrete spatial Fourier transform modified with time-dependent wavenumbers. In section 3.2, particular ODEs for free evolution are derived using the terminal condition for complex diffusion. In section 3.3, the adaptation for semi-free evolution is described.

3.1. Derivation of the general evolution equations

3.1.1. The ansatz

The proposed ansatz to transform the partially scaled CGLe (2.1) in wavenumber space is

$$\Psi = (1/W_1)\sum_{n=1}^{N} A_n(T)\exp\left[i\sigma\Theta_n(X, T)\right] \qquad \Theta_n = \phi_n(X, T) + \Phi_n(T)$$
$$\phi_n = K_n(T)(X - X_0) \qquad K_n(T) = (n - M)q + K_M(T) \qquad \sigma = \pm 1 \tag{3.1}$$

The spectral components are identified by indices, n, in the range $1 \leqslant n \leqslant N$, where N is the total number of components. A_n, K_n and Θ_n represent the amplitudes, wavenumbers and phases of the components, q is the wavenumber width of the components, M is the index of the component with the maximum amplitude, and W_1 is a normalisation factor determined by requiring that the dynamics remain unchanged as $N \to \infty$. In contrast to (2.8), the spectrum is generally asymmetric. During evolution, the component with the maximum amplitude

may change, in which case M changes to the index of the new such component at the next timestep in a numerical solution. The ansatz (3.1) is an approximation that becomes more accurate for narrow, single-peaked spectra, which are typical in solutions of the CGLe (the unscaled initial spectral width is $O(\varepsilon)$).

The purpose of σ is to include both complex conjugate forms of the total wave, i.e. the modulation combined with the base wave. The terminal condition determines the sign of σ (section 3.2.3). The expressions for the total wave and its components are

$$\begin{gathered}\Psi \exp\left[i\sigma\left\{k_r(X-X_0)-\omega_r T\right\}\right] \quad \textit{Total wave} \\ (A_n/W_1)\exp\left[i\sigma\left\{(k_r+K_n)(X-X_0)-\omega_r T+\Phi_n\right\}\right] \quad \textit{Total wave, Component } n\end{gathered} \tag{3.2}$$

The total wave (3.2) describes travelling and lengthening waves (section 3.2.6), whereas (2.8) describes standing waves.

3.1.2. Solution procedure

The procedure for deriving the general evolution equations starts by substituting (3.1) in the CGLe (2.1). From the resulting equation, ODEs for the evolution of A_n and $\Phi_n - \Phi_M$ are derived, containing variables that are functions of T only. Both Φ_M and K_M remain undetermined by this general solution. Making the substitution yields

$$\begin{aligned}&\sum_{n=1}^{N}\left[\left\{dA_n/dT-(L_{1n}+i(L_{2n}-\sigma\partial\Theta_n/\partial T))A_n\right\}\exp\left(i\sigma(\phi_n+\Phi_n)\right)\right] \\ &\quad+(1/W_2)(\mu_r-i\mu_i)\sum_{1\leqslant j,l,m\leqslant N}A_jA_lA_m\exp\left(i\sigma(\phi_{jlm}+\Phi_{jlm})\right)=0\end{aligned} \tag{3.3}$$

where W_2 is another normalisation factor. The identity $|\Psi|^2\Psi=\Psi^2\Psi^*$ is used to derive the nonlinear term in (3.3), and the summation is defined by

$$\sum_{1\leqslant j,l,m\leqslant N}=\sum_{j=1}^{N}\sum_{l=1}^{N}\sum_{m=1}^{N} \tag{3.4}$$

The linear expressions L_{1n}, L_{2n} and the phase terms ϕ_{jlm}, Φ_{jlm} are defined by

$$L_{1n}=\gamma_r-\alpha_r((n-M)q+K_M)^2 \tag{3.5}$$

$$L_{2n}=\gamma_i-\alpha_i((n-M)q+K_M)^2 \tag{3.6}$$

$$\phi_{jlm}=\phi_j+\phi_l-\phi_m=((j+l-m-M)q+K_M)(X-X_0) \tag{3.7}$$

$$\Phi_{jlm}=\Phi_j+\Phi_l-\Phi_m \tag{3.8}$$

The aim is to express (3.3) in the form

$$\sum_{n=1}^{N}\left[\left\{H_{1n}(T)+iH_{2n}(T)+iH_3(X,T)\right\}A_n\exp\left(i\sigma\Theta_n\right)\right]=0 \tag{3.9}$$

where the subscripted H are expressions containing real variables. Equation (3.9) then yields $H_{1n}=0$ and $H_{2n}=0$ for $1\leqslant n\leqslant N$ which are $2N$ evolutionary ODEs, and $H_3=0$ which, after inclusion of the auxiliary conditions, determines the characteristic lines.

For (3.3) to conform to (3.9), a subset of the nonlinear terms in the second summation in (3.3) is grouped within the first summation. This subset has combinations of j, l and m that satisfy

$$\phi_{jlm}=\phi_n \qquad \textit{for } 1\leqslant j,\ l,\ m,\ n\leqslant N \tag{3.10}$$

From (3.1) and (3.7), this condition requires

$$j+l-m=n \qquad \textit{for } 1\leqslant j,\ l,\ m,\ n\leqslant N \tag{3.11}$$

This grouping accounts for all nonlinear terms with values of j, l and m in the range $1\leqslant j+l-m\leqslant N$. The other nonlinear terms give n outside this range and are ignored. Equations (3.10) and (3.11) are substituted in (3.3), resulting in the following equation

$$\sum_{n=1}^{N}\left[\left\{\frac{1}{A_n}\left(\frac{dA_n}{dT}-g_n\right)+i\left(\sigma\frac{\partial\Theta_n}{\partial T}-f_n\right)\right\}A_n\exp\left(i\sigma\Theta_n\right)\right]=0 \tag{3.12}$$

where

$$g_n(T)=L_{1n}A_n-(\mu_rS_{Cn}+\mu_iS_{Sn})/W_2 \qquad \textit{for } 1\leqslant n\leqslant N \tag{3.13}$$

$$f_n(T)=L_{2n}+(\mu_iS_{Cn}-\mu_rS_{Sn})/(W_2A_n) \qquad \textit{for } 1\leqslant n\leqslant N \tag{3.14}$$

$$S_{Cn} = \sum_{\substack{j+l-m=n \\ 1\leqslant j,l,m\leqslant N}} A_j A_l A_m \cos \Phi_{jlmn} \qquad S_{Sn} = \sum_{\substack{j+l-m=n \\ 1\leqslant j,l,m\leqslant N}} A_j A_l A_m \sin \Phi_{jlmn} \tag{3.15}$$

$$\Phi_{jlmn} = \Phi_j + \Phi_l - \Phi_m - \Phi_n \tag{3.16}$$

The summations in (3.15) are defined by (3.4) with the terms restricted by (3.11). Later in the analysis Θ_n and Φ_n are expressed relative to the phase of component M. These relative phases are denoted by Θ_{nM} and Φ_{nM} and are defined by

$$\Theta_{nM} = \Theta_n - \Theta_M \qquad \Phi_{nM} = \Phi_n - \Phi_M \tag{3.17}$$

Equation (3.16) can be expressed in terms of the relative phases

$$\Phi_{jlmn} = \Phi_{jM} + \Phi_{lM} - \Phi_{mM} - \Phi_{nM} \tag{3.18}$$

where Φ_{jM}, Φ_{lM} and Φ_{mM} are defined similarly to (3.17). Two relations used later follow from (3.1)

$$\Theta_{nM} = (n - M)q(X - X_0) + \Phi_{nM} \tag{3.19}$$

and therefore

$$\partial\Theta_{nM}/\partial T = d\Phi_{nM}/dT \tag{3.20}$$

3.1.3. The ancillary function, F_M, and the general solution

Equation (3.12) is not yet in the required form of (3.9) because $\partial\Theta_n/\partial T$ are dependent on X from (3.1). This problem is overcome by reformulating (3.12) in terms of differentials of the relative phases, $\partial\Theta_{nM}/\partial T$, which are independent of X as shown by (3.20). To accomplish this reformulation, the following expression (3.21) is added to (3.12) within the summation sign and then subtracted as a separate group

$$\sum_{n=1}^{N} [i(\partial F_M/\partial T - \sigma\partial\Theta_M/\partial T)A_n \exp(i\sigma\Theta_n)] \tag{3.21}$$

In (3.21), $F_M(X,\ T)$ is a general function of X and T, and is termed the 'ancillary function'. After this reformulation, (3.12) becomes

$$\sum_{n=1}^{N}\left[\left\{\frac{1}{A_n}\left(\frac{dA_n}{dT} - g_n\right) + i\left(\sigma\frac{\partial\Theta_{nM}}{\partial T} + \frac{\partial F_M}{\partial T} - f_n\right)\right\}A_n \exp(i\sigma\Theta_n)\right] - i\left(\frac{\partial F_M}{\partial T} - \sigma\frac{\partial\Theta_M}{\partial T}\right)\sum_{n=1}^{N} A_n \exp(i\sigma\Theta_n) = 0 \tag{3.22}$$

Equation (3.22) now has the form of (3.9) and is solved by equating the individual terms under the first summation sign to zero, giving

$$dA_n/dT = g_n \qquad \text{for } 1 \leqslant n \leqslant N \tag{3.23}$$

$$d\Phi_{nM}/dT = \sigma(f_n - f_M) \qquad \text{for } 1 \leqslant n \leqslant N,\quad n \neq M \tag{3.24}$$

$$\partial F_M/\partial T = f_M \tag{3.25}$$

where (3.20) and (3.25) are used to derive (3.24). These constitute $2N$ evolution equations for the $2N$ variables A_n, $\Phi_{nM\,(n\neq M)}$ and F_M for $1 \leqslant n \leqslant N$. The final term of (3.22) is also required to be zero, i.e. $\partial F_M/\partial T = \sigma\partial\Theta_M/\partial T$. From (3.1), this requirement can be written as

$$\frac{\partial F_M}{\partial T} = \sigma(X - X_0)\frac{dK_M}{dT} + \sigma\frac{d\Phi_M}{dT} \tag{3.26}$$

Equation (3.26) expresses a condition that must be satisfied for the evolution equations (3.23–3.25) to be valid.

Equations (3.23–3.25) are the general evolution equations derived from the ansatz (3.1). K_M, Φ_M and σ remain undetermined in this general solution. To derive a particular solution, F_M needs to be expressed as a unique function of K_M such that the validity condition (3.26) is met. The evolution equation for K_M then follows from (3.25). This procedure requires auxiliary conditions that are specific to an application. Section 3.2 describes the procedure for free evolution.

3.2. Derivation of the particular equations for free evolution

3.2.1. Deriving the relation of F_M to K_M

The particular equations for free evolution are derived from three conditions that determine the ancillary function F_M as a function of the wavenumber K_M. The third condition is the terminal condition for complex diffusion, which is specific to free evolution.

(1) The functional dependence, $F_M(X,\ T,\ K_M(T)(X - X_0))$, is a requirement for $K_M(T)$ to signify a wavenumber (the general form, $F_M(X,\ T,\ K_M(T))$, implies no specific meaning for $K_M(T)$). Without losing generality, F_M is expressed as a function of another general function $F_1(X,\ T)$ added to $K_M(T)(X - X_0)$. This form facilitates the derivation of F_M.

$$F_M(F_1(X,\ T) + K_M(T)(X - X_0)) \qquad \textit{Functional dependence of } F_M \tag{3.27}$$

(2) From (3.25) and (3.14) for $n = M$, $\partial F_M/\partial T$ depends on T only, and therefore F_M has the form

$$F_M = F_2(T,\ K_M(T)) + F_3(X - X_0) \tag{3.28}$$

where $F_2(T,\ K_M(T))$ and $F_3(X - X_0)$ are general functions.

(3) For free evolution, the terminal condition requires that after K_M reduces to $-k_r$, it remains at this value

$$dK_M/dT = 0 \quad \textit{when} \quad K_M = -k_r \tag{3.29}$$

and the spectrum is truncated to exclude components having $K_n < -k_r$.

Conditions (3.27) and (3.28) state that F_M is both a function of the product of $K_M(T)$ and $X - X_0$, and the sum of separate functions of $K_M(T)$ and $X - X_0$. To satisfy both conditions requires F_M to be a logarithmic function with, for generality, a multiplying constant. Thus, from (3.27)

$$F_M = C_M \ln(F_1(X,\ T) + K_M(T)(X - X_0)) \tag{3.30}$$

where C_M is a real constant. For F_M to satisfy (3.28), F_1 must have the form $F_4(T)(X - X_0)$ or $K_M(T)F_5(X - X_0)$ where $F_4(T)$ and $F_5(X - X_0)$ are general functions. A similar analysis to that below shows the latter form for F_1 is incompatible with (3.29). Substituting the first form for F_1 in (3.30), F_M becomes

$$F_M = C_M\{\ln(F_4(T) + K_M(T)) + \ln(X - X_0)\} \tag{3.31}$$

Equation (3.31) has the required form of (3.28). The next step is to set F_4 using the terminal condition (3.29). Differentiating (3.31) with respect to T and incorporating (3.29) yields

$$(F_4 - k_r)\partial F_M/\partial T = C_M dF_4/dT \tag{3.32}$$

To satisfy (3.32) for any value of C_M requires $F_4 = k_r$. The terminal condition, but not the terminal time, is specified as an auxiliary condition. Because the terminal time is unknown, the constraint imposed by the terminal condition on the general solution (in this case, $F_4 = k_r$) applies at all times. Substituting $F_4 = k_r$ in (3.31) gives the sought relation of F_M to K_M

$$F_M = C_M\{\ln(k_r + K_M(T)) + \ln(X - X_0)\} \tag{3.33}$$

where $K_M \geqslant -k_r$.

3.2.2. The evolution equation for K_M

Differentiating F_M with respect to T in (3.33) gives

$$\frac{\partial F_M}{\partial T} = \frac{C_M}{k_r + K_M}\frac{dK_M}{dT} \tag{3.34}$$

The evolution equation for K_M is derived from (3.34) and (3.25)

$$\frac{dK_M}{dT} = \frac{(k_r + K_M)f_M}{C_M} \tag{3.35}$$

The sign of C_M provides two solutions, for diffusive evolution when $dK_M/dT < 0$ and antidiffusive evolution when $dK_M/dT > 0$. The terminal condition allows only the diffusive solution, which requires C_M to have the opposite sign to f_M

$$f_M/C_M < 0 \qquad \textit{for diffusive evolution} \tag{3.36}$$

3.2.3. The characteristic equation

The validity condition (3.26) needs to be satisfied. A comparison of (3.34) with (3.26) determines two properties of the solution. Firstly, Φ_M is constant with respect to time

$$d\Phi_M/dT = 0 \tag{3.37}$$

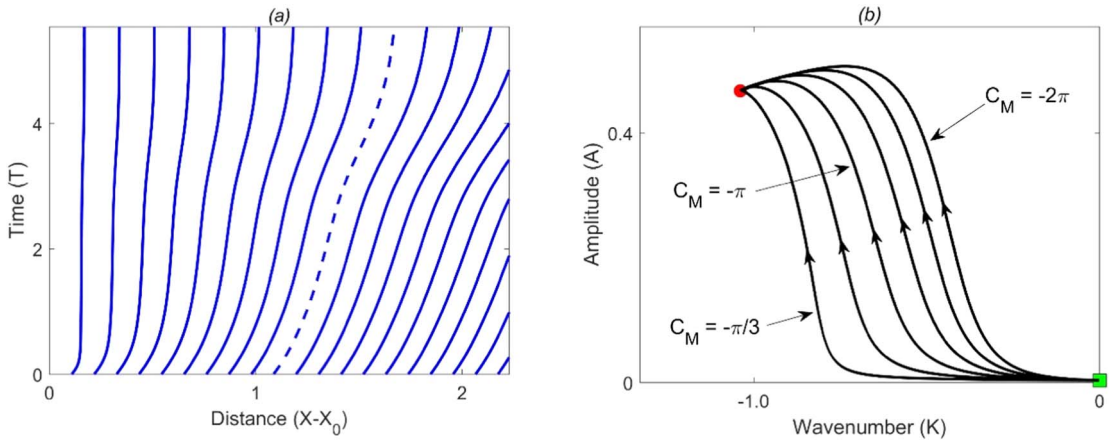

Figure 2. Evolution from a perturbed $\Psi = 0$ state (centred on the green square in b) towards a sideband-stable SFP state (red circle in b) computed from (A6) and (A8). (a, left) Characteristic lines defined by (3.38) in X, T space for equal increments of C_M, with $X > X_0$ and $\sigma = -1$. The dashed line has $C_M = -\pi$. Characteristic lines for $X < X_0$ show reflection symmetry about $X = X_0$. Distance: computed from (3.39). Time: computational timestep multiplied by number of timesteps. (b, right) Evolution of component M in K, A space for six characteristic lines for $C_M = -\pi/3$ to -2π at intervals of $-\pi/3$. Spectral evolution for $C_M = -\pi$ is shown in figure 1(b) and the video (appendix C). The equation constants simulate the experiment in section 4: $\alpha_r = 0.39$, $\alpha_i = 0.86$, $\gamma_r = 1.62$, $\gamma_i = 0.69$, $\mu_r = 5.48$, $\mu_i = 1.08$, $k_r = 2.89$.

This property and the initial condition determine Φ_M. Secondly, $C_M/(k_r + K_M)$ is required to satisfy

$$\sigma(X - X_0) = C_M/(k_r + K_M) \tag{3.38}$$

Equation (3.38) shows there is a family of solutions for different values of C_M. Each value of C_M corresponds to a line in the X, T plane along which the solution evolves. These lines are analogous to the characteristic lines in, for example, solutions to hyperbolic PDEs. In the present case, they describe constant values of the spatial part of the total wave phase for component M, (3.2). For a given characteristic line, the value of C_M is determined from the initial state. For this state, $K_M(0) = 0$ and X_{in} is the initial value of X for the characteristic line

$$C_M = \sigma k_r (X_{in} - X_0) \tag{3.39}$$

Figure 2(a) shows an example of the characteristic lines.

The sign of σ (defined as ± 1 in (3.1)) is determined by the requirement that the solutions evolve diffusively (not antidiffusively). If $f_M > 0$, it follows from (3.36) that $C_M < 0$ and therefore from (3.38) that $\sigma(X - X_0) < 0$. Similarly, if $f_M < 0$, it follows that $C_M > 0$ and $\sigma(X - X_0) > 0$. Thus, σ is determined by

$$\sigma = -\mathrm{sgn}(f_M(X - X_0)) = \mathrm{sgn}(C_M(X - X_0)) \tag{3.40}$$

3.2.4. Summary and numerical solution of the free evolution equations

Equations (3.23), (3.24) and (3.35) are $2N$ coupled, first-order ODEs describing the evolution of the $2N$ variables, A_n, $\Phi_{nM(n\neq M)}$ and K_M for $1 \leqslant n \leqslant N$ along each characteristic line defined by C_M. These ODEs can be solved numerically by a timestepping algorithm, such as a Runge–Kutta method. After the $2N$ variables are calculated at each timestep, Θ_{nM} is determined by (3.19), Φ_M by (3.37), and $K_{n(n\neq M)}$ and Ψ by (3.1). The location in physical space relative to X_0 is determined by the characteristic equation (3.38). M is updated if the component with maximum amplitude changes.

A numerical solution of the evolution equations requires that the normalisation factors W_1 in (3.1) and W_2 in (3.13) and (3.14) are determined. For W_2, there are coherent nonlinear terms (for which $\Phi_{jlmn} = 0$) that need to be considered separately from the non-coherent terms. These issues are addressed in appendix A. The evolution equations (3.23), (3.24) and (3.35) are simplified if only the coherent nonlinear terms are included, resulting in (A6)–(A8).

Figure 2(a) shows a set of characteristic lines in X, T space and figure 2(b) shows the evolution of component M in K, A space along different characteristic lines.

3.2.5. The fixed point, X_0

The point X_0 is a fixed point from which the modulated waves lengthen to each side. The location of X_0 is determined by application-specific properties such as details of the perturbation in the initial state. For some long domains, a single fixed point would require long-range spatial correlations during evolution that might be physically unrealistic, especially in the early stages. Such domains are conjectured to have two or more

subdomains, each with a fixed point determined by spatial variations in the initial perturbation. These subdomains would be separated by short transition regions for continuity of the total wave. Experimental identification of single or multiple fixed points requires further research.

3.2.6. Kinematic properties and the dispersion equation

Some kinematic properties are obtained from this analysis. The dispersion equation for a general component, n, is given by

$$\Omega_n = -\frac{\partial \Theta_n}{\partial T} = -(X - X_0)\frac{dK_n}{dT} - \frac{d\Phi_n}{dT} = -\sigma f_n \tag{3.41}$$

where (3.1), (3.17), (3.24), (3.35), (3.37) and (3.38) are used. The phase velocity v_n is derived as

$$v_n = -\frac{\partial \Theta_n/\partial T}{\partial \Theta_{n,tot}/\partial X} = -\frac{\sigma f_n}{k_r + K_n} \tag{3.42}$$

where $\Theta_{n,tot}$ is the total wave phase for component n, (3.2). Since f_n/ω_r is $O(\varepsilon^2)$, v_n is slow compared with the base wave phase velocity. Equation (3.41) is the sum of the wave frequencies resulting from the lengthening of waves and the travelling waveform. The separate expressions for the lengthening (subscript 'le') and travelling (subscript 'tr') wave frequencies and phase velocities are

$$\Omega_{n,le} = -(X - X_0)\frac{dK_n}{dT} = -\sigma f_M \qquad v_{n,le} = -\frac{\sigma f_M}{k_r + K_n} \tag{3.43}$$

$$\Omega_{n,tr} = -\frac{d\Phi_n}{dT} = -\sigma(f_n - f_M) \qquad v_{n,tr} = -\frac{\sigma(f_n - f_M)}{k_r + K_n} \tag{3.44}$$

There are two competing processes that determine the lengthening frequency $\Omega_{n,le}$. This frequency increases with distance from X_0 owing to the lengthening of waves but decreases with distance because of the slower rate at which the wavenumber evolves. These effects cancel each other, resulting in no explicit dependence of $\Omega_{n,le}$ on $X - X_0$ or dK_n/dT. There is an implicit dependence on these parameters because f_M is a function of K_M, which evolves at different rates according to the value of C_M.

Equations (3.43) and (3.40) show that the lengthening phase velocity is always directed away from X_0. Equation (3.44) with $n = M$ shows that the travelling frequency and phase velocity for component M are zero. In summary, the total wave consists of a fast travelling wave (the base wave) combined with a modulation that slowly lengthens in both directions away from X_0, in which component M is non-travelling and the other components travel slowly in a direction determined by the sign of $-\sigma(f_n - f_M)$.

The dispersion equation (3.41) has the same functional form as for the bounded evolution equations (for which the auxiliary conditions include $dK_M/dT = 0$ for all T). For bounded evolution, $\Omega_n = -\partial\Theta_n/\partial T = -\sigma f_n$, which follows directly from (3.12) because $\partial\Theta_n/\partial T$ are now independent of X. Although the form of Ω_n is the same for bounded and free evolution, the contributions of the wave lengthening and travelling processes are different (for bounded evolution there is no wave lengthening, i.e. $\Omega_{n,le} = 0$ and $\Omega_{n,tr} = -\sigma f_n$).

3.2.7. Symmetry properties

The particular solution for free evolution has no undetermined constants or functions apart from some simple symmetries. These are (1) translational symmetry in space and time, (2) scaling symmetry (section 2.1), (3) Galilean symmetry (appendix B) and (4) reflection symmetry about X_0 (sections 3.2.3, 3.2.5 and figure 2(a)).

There is no reflection symmetry in the sense that an identical counter-propagating wave at a given location and time cannot exist. The particular solution for bounded evolution has phase symmetry [6] but for free evolution this symmetry is broken. In the latter case, the validity condition (3.26) couples Φ_M to the other evolution equations, whereas for bounded evolution there is no validity condition and Φ_M is isolated.

3.2.8. Uniqueness of the particular solution

A demonstration of the uniqueness of (3.33) for F_M is not attempted but a plausible alternative solution is rejected. The following forms of F_M and F_1 in (3.27) satisfy (3.28) and the terminal condition (3.29) for finite values of the exponent, p

$$F_M = C_M \ln(F_1(X, T) - (-K_M(T))^p(X - X_0)^p) \qquad F_1 = k_r^p(X - X_0)^p \tag{3.45}$$

However, (3.45) gives rise to an unrealistic initial condition, which is apparent from the derived characteristic equation

$$\sigma(X - X_0) = C_M p(-K_M)^{p-1}/(k_r^p - (-K_M)^p) \tag{3.46}$$

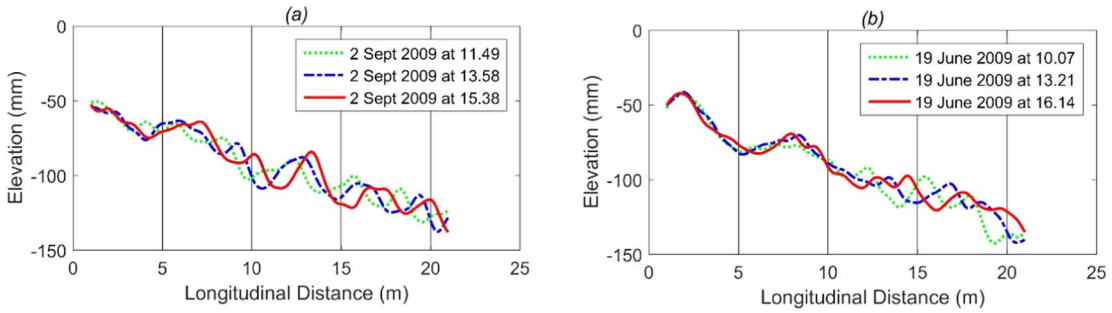

Figure 3. Bed level profiles along one side of the channel at three times (see legends) in the experiments of [21, 22]. (a, left) An experiment in which the bed at the upstream boundary is maintained at a fixed level (−49 mm elevation). (b, right) A separate experiment in which a vertical plate at the upstream boundary extends from one side into the channel. See the text of section 4 for a description and interpretation of these figures. Figures 3(a) and 3(b) are redrawn from figures 11 and 8 respectively in [21].

This equation shows that, for the initial state in which $K_M(0) = 0$, finite values of C_M are possible only for $p = 1$. The solutions for some complex diffusion equations other than the CGLe have $k_r = 0$ and K_M replaced by k_M (section 5). For these solutions, (3.45) and (3.46) reduce to the case for $p = 1$ with the characteristic constant $C_M p$.

3.3. Semi-free evolution

The derivation of the semi-free evolution equations follows section 3.2, with the location of X_0 set at the single boundary and with differences to some auxiliary conditions. The terminal condition stands, but a different initial condition applies and there is a boundary condition at X_0. The boundary condition relates to the total wave.

The following example is for a boundary condition in which the total wave (3.2) is held at a time-constant value of zero at X_0. This corresponds to the upstream boundary condition in the experiment outlined in section 4. This boundary condition can be satisfied either by fixing the amplitude to zero or by fixing the total wave phase at a nodal value. The latter case is consistent with the ansatz (3.1) and allows for unrestricted amplitude growth near the boundary. However, a standing wave arising from reflections between two boundaries cannot occur. For this example, the only possibility to satisfy the boundary condition is a travelling wave whose total phase velocity is zero.

The initial total wavenumber is determined from the dispersion equation for the initial state, setting the total wave frequency to zero. Such a wave is represented by a single component, M. Its amplitude and wavenumber evolve according to (3.23) and (3.35) respectively, provided it is unstable in the initial state. During evolution, the travelling phase velocity remains at zero as shown by (3.44) for $n = M$, which is consistent with the boundary condition. The rate of amplitude growth is generally slower than that of the wavenumber component, K_M, in free evolution.

4. Qualitative evidence from channel sandbar experiments

Qualitative experimental evidence for the free and semi-free evolution equations (3.23), (3.24) and (3.35) is presented in this section. Several experiments have been conducted in different laboratories on the evolution of sandbars in straight channels in which the bars evolve alternately on each side of the channel [18–22]. In these experiments, energy was transferred into the channel by water flow driven by gravity over a sand layer on a gentle downslope. The experiments had different constraints at the upstream boundary, such as a fixed bed level or a partial barrier to create a stronger locally perturbed flow. Water and sediment leaving the channel at the downstream end were collected and recirculated. The CGLe has been derived as a nonlinear evolution equation for the bars on long time and space scales [17]. The experiments were designed to be just beyond the critical state for instability of a uniform channel bed, and theoretically had sideband-stable SFP final states for the bars.

A quantitative comparison of predictions by the free and semi-free evolution equations with the experimental data is beyond the scope of this study. The purpose of this section is to compare qualitatively two observed phenomena with predictions by these equations and by the solution for bounded evolution, (2.9). The first phenomenon is that two bar types evolved in different regions of the channel. Non-travelling bars evolved near the upstream boundary and travelling bars evolved further downstream. The second phenomenon is that, for both bar types, the bar wavelengths increased with time as the bars grew in amplitude. The first phenomenon is qualitatively described by the semi-free solution for the non-travelling bars near the upstream boundary, and

by the free solution for the travelling bars further downstream. The solution for bounded evolution predicts a single bar type throughout the channel and therefore does not agree qualitatively with the observation of the two bar types. The second phenomenon, the increase in bar wavelengths with time, is qualitatively predicted by (3.35) for free and semi-free evolution. However, the solution for bounded evolution predicts that the wavelength of the spectral peak remains unchanged from its initial value (section 2.4, figure 1 and the video in appendix C).

Figure 3(a) shows the measurements of bed level profiles along one side of the channel from an experiment reported in [21, 22]. These measurements were made at three different times, approximately two hours apart. The bed at the upstream end was maintained at a fixed level. In the interior (longitudinally) of the channel, the three measured profiles are out of phase indicating that the bars behave as travelling waves (termed 'free bars' in [23]). The bars in this region grew to reach a maximum amplitude in about 1–2 days. Close to the upstream boundary the three measured profiles are approximately in phase indicating that the bars behave as non-travelling waves (termed 'hybrid bars' in [23]). Their amplitudes grew more slowly than those of the free bars and continued to increase after tens of days. Between the two types of bars is a narrow transition region at approximately 6–7 m. The free and hybrid bar regions correspond to the application of the free and semi-free evolution equations respectively.

In both regions, the bar wavelengths increased as the bars grew in amplitude. In the upstream boundary region, the measured hybrid bar wavelengths increased by a factor of approximately 1.07 during evolution. For the free bars in the channel interior, measurements near full development of the bars showed that the bar wavelengths were approximately 1.5 times longer than the wavelength of the theoretical initially fastest growing component.

Another study [18] presented the results of nine separate experiments on free bar evolution. For each experiment, measurements of free bar wavelengths were made between four and seven different times during the growth of the bars. These measurements showed that the free bar wavelengths increased by factors between 1.3 and 5.3 from the first measured states to the full development of the bars.

Returning to the experiments of [21, 22], figure 3(b) refers to an identical experiment to that for figure 3(a) but with a vertical metal plate at the upstream end, extending transversely from one side for about two-thirds of the channel width. This experiment also had hybrid (non-travelling) bars near the upstream boundary and free (travelling) bars in the interior region, separated by a narrow transition region at approximately 11–12 m. The interior region is qualitatively described by the free solution, but the boundary region is less well described by the CGLe because of the strong flow perturbation caused by the plate. This resulted in an upstream boundary region that was longer and had a faster growing hybrid bar amplitude than shown in figure 3(a), although the hybrid bar wavelengths were similar.

5. Free evolution in other complex diffusion equations

5.1. The complex heat equation

In section 3, the free evolution equations for the CGLe are derived using the terminal condition for complex diffusion as an auxiliary condition. This suggests that a similar procedure can be used to derive free evolution equations for other time-dependent PDEs with a complex or imaginary diffusion term. One such PDE is the complex heat equation

$$\partial\Psi/\partial T = (\alpha_r + i\alpha_i)\partial^2\Psi/\partial X^2 \tag{5.1}$$

For the analysis in sections 5.1 and 5.2, Ψ represents an unscaled, unmodulated wave. All variables are unscaled and the subscript u is dropped for clarity. The initial condition is a finite value of Ψ and there is no restriction on the wavenumber range. For a real diffusion coefficient, there are two main methods to solve (5.1); see, for example, [3]. These use a Fourier integral transform for an unbounded spatial domain, and a separation of space-dependent and time-dependent variables for a bounded domain. A unified approach was presented in [24] with the two methods as special cases. For a complex diffusion coefficient, the same methods can be used if the auxiliary conditions require a solution with time-constant wavenumbers. In [25], a solution for such cases was obtained using the Fourier integral method.

The present study provides a third method for solving (5.1), which applies to free or semi-free evolution with time-dependent wavenumbers. The procedure follows sections 2 and 3, adapted by setting the CGLe constants for non-diffusive processes to zero ($\gamma_r = \gamma_i = \mu_r = \mu_i = 0$) and employing unscaled variables. Unmodulated wavenumbers and frequencies are used (k_n and ω_n replace K_n and Ω_n, with $k_r = 0$ and $\omega_r = 0$). Because the complex heat equation is linear, the spectral components are treated as linearly independent. Consequently, the ansatz (3.1) is modified such that the relation $k_n(T) = (n - M)q + k_M(T)$ does not apply for $T > 0$. This removes the approximation in (3.1). Incorporating these changes, the analysis in section 3.1 yields (3.12) with g_n and f_n given by

$$g_n(T) = -\alpha_r A_n k_n^2 \qquad f_n(T) = -\alpha_i k_n^2 \tag{5.2}$$

Separate ancillary functions $F_n(X,\ T)$ are defined for each spectral component. The expression (5.3) is added within the summation sign in (3.12) and then subtracted as a separate group.

$$\sum_{n=1}^{N} [i(\partial F_n/\partial T - \sigma \partial \Theta_n/\partial T) A_n \exp(i\sigma\Theta_n)] \tag{5.3}$$

This yields the general evolution equations

$$dA_n/dT = g_n \qquad \partial F_n/\partial T = f_n \qquad for\ 1 \leqslant n \leqslant N \tag{5.4}$$

with the validity conditions

$$\frac{\partial F_n}{\partial T} = \sigma(X - X_0)\frac{dk_n}{dT} + \sigma\frac{d\Phi_n}{dT} \qquad for\ 1 \leqslant n \leqslant N \tag{5.5}$$

The ODEs for free evolution are derived by applying the analysis in section 3.2 to each spectral component. The subscript M in section 3.2 is replaced by n for $1 \leqslant n \leqslant N$. In particular, the terminal condition (3.29) becomes $dk_n/dT = 0$ when $k_n = 0$. The following evolution equations are derived

$$dk_n/dT = -\alpha_i k_n^3/C_n \qquad dA_n/dT = -\alpha_r A_n k_n^2 \qquad d\Phi_n/dT = 0 \qquad for\ 1 \leqslant n \leqslant N \tag{5.6}$$

The sign of each C_n is chosen such that $dk_n/dT < 0$. These equations have the solution

$$k_n = k_{n0}/(1 + p_{1n}T)^{1/2} \qquad A_n = A_{n0}/(1 + p_{1n}T)^{p_{2n}} \qquad \Phi_n = \Phi_{n0}$$
$$p_{1n} = 2k_{n0}^2\alpha_i/C_n \qquad p_{2n} = \alpha_r C_n/(2\alpha_i) \qquad for\ 1 \leqslant n \leqslant N \tag{5.7}$$

where the constants of integration are set by the initial values of wavenumber, amplitude and phase, k_{n0}, A_{n0} and Φ_{n0}. The solution for each component has separate characteristic lines. The power-law decay of amplitude with time contrasts with the exponential decay that occurs for a real diffusion coefficient. For each component, $\omega_n = \omega_{n,le} = -\sigma f_n$ and $\omega_{n,tr} = 0$, which indicates that the waves are lengthening and non-travelling.

5.2. The linear free Schrödinger equation

The heat equation with an imaginary diffusion term is identical to the time-dependent Schrödinger equation in the absence of external constraints (the free Schrödinger equation). In quantum mechanics, this equation describes the evolution of the wavefunction for a free non-relativistic particle, and has a plane-wave particular solution. In classical mechanics, the free Schrödinger equation has a different particular solution because the auxiliary conditions include the terminal condition for a classical physical process (complex diffusion). For an initial plane wave with amplitude A_{M0} and wavenumber k_{M0}, the method described in section 5.1 yields the solution (5.7) with $\alpha_r = 0$ and $n = M$. The wavenumber decreases with time according to (5.7), during which the amplitude remains constant. In classical mechanics, the diffusion term in the free Schrödinger equation acts to lengthen an initial plane wave.

5.3. The nonlinear Schrödinger equation (NLSe)

The NLSe is a special case of the CGLe with $\gamma_r = \gamma_i = \mu_r = \alpha_r = 0$, [1–3]

$$\partial\Psi/\partial T = i\alpha_i \partial^2\Psi/\partial X^2 + i\mu_i|\Psi|^2\Psi \tag{5.8}$$

The NLSe can describe narrow spectral modulations of a plane base wave, but the initial condition and the physical interpretation of some parameters differ from the CGLe. Variables are scaled as in sections 2 and 3, but Ψ has a finite initial value and ε represents a small amplitude parameter such as the initial wave steepness. The following analysis concerns the free evolution of a plane base wave with a general initial amplitude $A_M = A_{M0}$, phase $\Phi_M = \Phi_{M0}$, wavenumber $K_M = 0$ and total wavenumber $k_M = k_r$. Incorporating the stated changes, the derivation in section 3 shows that K_M decreases with time while A_M and Φ_M remain constant at A_{M0} and Φ_{M0}. From (3.35) and (3.14), the evolution equation for K_M is

$$dK_M/dT = \alpha_i(k_r + K_M)(p_3^2\,\mathrm{sgn}(\xi) - K_M^2)/C_M \qquad p_3 = |\xi|^{1/2}A_{M0} \qquad \xi = \mu_i/\alpha_i \tag{5.9}$$

The sign of C_M is chosen such that $dK_M/dT < 0$. Three solutions are derived for $\xi > 0$ and $k_r > p_3$ in (5.10), $\xi > 0$ and $k_r < p_3$ in (5.11), and $\xi < 0$ in (5.12), using the definitions in (5.13). The constants of integration are set by the initial wavenumber, $K_M = 0$.

$$(1 + K_M/k_r)^{-1}(1 + K_M/p_3)^{p_4}(1 - K_M/p_3)^{p_5} = \exp(\beta_1 T) \qquad \xi > 0 \quad k_r > p_3 \tag{5.10}$$

$$(1 + K_M/k_r)(1 + K_M/p_3)^{-p_4}(1 - K_M/p_3)^{-p_5} = \exp(\beta_2 T) \qquad \xi > 0 \quad k_r < p_3 \tag{5.11}$$

$$(1 + K_M/k_r)(1 + K_M^2/p_3^2)^{-1/2}\exp[(k_r/p_3)\tan^{-1}(K_M/p_3)] = \exp(\beta_3 T) \qquad \xi < 0 \tag{5.12}$$

$$p_4 = (p_3 + k_r)/2p_3 \qquad p_5 = (p_3 - k_r)/2p_3$$
$$\beta_1 = \alpha_i(k_r^2 - p_3^2)/C_M \qquad \beta_2 = \alpha_i(p_3^2 - k_r^2)/C_M \qquad \beta_3 = -\alpha_i(p_3^2 + k_r^2)/C_M \tag{5.13}$$

As $T \to \infty$, these solutions give $K_M \to -p_3$ for (5.10) and $K_M \to -k_r$ for (5.11) and (5.12). The dispersion equation is $\Omega_M = \Omega_{M,le} = -\sigma f_M$, indicating a lengthening and non-travelling wave.

Much theoretical interest concerns the modulations that develop from an initial, sideband-unstable, stationary plane base wave. This study shows that an external constraint, such as a spatial boundary condition, is required to maintain a plane wave as stationary. In free evolution, a plane wave is generally non-stationary, irrespective of sideband stability. The wavenumber of a sideband-stable plane wave evolves according to (5.10)–(5.12). For a sideband-unstable plane wave, modulations develop in combination with the wavenumber evolution.

6. Discussion

This study has derived freely evolving solutions of nonlinear complex diffusion equations with sideband-stable SFP states (as well as linear equations). A future extension is to investigate analogous solutions with sideband-unstable SFP states. A related theoretical topic is to reconsider the stability criteria for SFP states, which were derived for bounded evolution in [5]. Because of the extra degree of freedom in free evolution, stability analyses of SFP states need to account for perturbations in K_M and A_M as well as in the sidebands, which would result in new stability conditions. Other theoretical topics could include an analysis of the transition regions between the free and semi-free solutions, and a proof of the uniqueness of (3.33) for F_M. Future reporting of quantitative comparisons with the channel sandbar experiments is planned.

The sandbar experiments have continuous forcing throughout the channel, and an upstream boundary condition whose influence persists for only a short distance (typically a few metres or one to two bar wavelengths). The physical causes of this limited spatial persistence require further study. The elastic properties of saturated granular material have been investigated [26, 27], but no research appears to have considered how the effects of boundary constraints decay with distance in a granular medium subjected to continuous and ubiquitous forcing. This issue is relevant for other material media with a similar type of forcing and sufficiently long spatial extent.

Other particular solutions of the CGLe have been extensively researched. A well-studied class of solutions describes localised coherent structures such as pulses or fronts embedded in regular solutions (e.g. plane waves or $\Psi = 0$) elsewhere in the spatial domain [1, 10–13]. For other solutions, boundary conditions have an essential role [9, 10]. Sideband-unstable systems can evolve to spatially extended turbulent or chaotic states [1, 4], or display convective instabilities [1, 14]. However, these solutions do not predict waves lengthening with time throughout the spatial domain, nor the qualitative features of the experiments outlined in section 4. An open question is, starting from a perturbed $\Psi = 0$ state or other physically realistic state, what criteria determine which of the many possible particular solutions of the CGLe is selected as the evolutionary path? In addition to the CGLe constants, relevant factors include the auxiliary conditions, domain length, material medium properties and details of the initial perturbation. The particular solutions for free and semi-free evolution derived in this study are possible outcomes.

7. Conclusions

New ordinary differential equations for the evolution of spectral components are derived from the complex Ginzburg–Landau equation. They apply to one-dimensional spatial domains without boundaries (free evolution) and with one fixed boundary (semi-free evolution). In physical applications, they are relevant to long domains. The semi-free evolution equations apply close to the boundaries where boundary conditions have an influence. The free evolution equations apply in the interior of the domains away from boundary effects. These evolution equations are contrasted with those previously derived for short spatial domains in which the boundary conditions have an influence that extends throughout the domains (bounded evolution).

The derivation uses a novel modification of a discrete spatial Fourier transform in which the wavenumber of the peak spectral component (denoted by its index, M) is time-dependent. The other components have wavenumbers fixed relative to M, implying that the spectrum as a whole evolves in wavenumber space. Particular solutions for free and semi-free evolution are derived using a novel auxiliary condition obtained from the terminal condition for complex diffusion (after wavenumbers evolve to zero, they remain at zero). The terminal condition requires that wavenumbers decrease with time. The outcome is a set of coupled, first-order ordinary differential equations for the evolution of the amplitude, wavenumber and phase of all spectral

components, applied along characteristic lines. A dispersion equation is derived that applies to lengthening waves as well as to travelling waves.

Laboratory experiments on the evolution of subaqueous channel sandbars show regions corresponding to free and semi-free evolution, and that the bar wavelengths increase with time as the bars grow in amplitude. The analysis applies to other complex diffusion equations, yielding new freely evolving solutions for the complex heat equation and Schrödinger equation (linear and nonlinear).

Acknowledgments

The author is grateful to Alessandra Crosato for providing support throughout this work and to Ralph Schielen and Arjen Doelman for helpful discussions about the CGLe.

Data availability statement

All data that support the findings of this study are included within the article (and any supplementary files).

Appendix A. Normalisation and coherent nonlinear terms for free evolution

Appendix A describes the procedure to determine the normalisation factor, W_2, for the nonlinear terms in the free evolution equations (3.23), (3.24) and (3.35). This requires calculating the number of distinct combinations of spectral components in the summations in S_{Cn} and S_{Sn} defined in (3.15), and ensuring that the dynamics remain unchanged as the number of components, $N \to \infty$. The normalisation factor W_1 in (3.1) is also determined.

A complication is that, during evolution, the amplitudes of some components can decay to zero (or close to zero). For example, for a system evolving towards a sideband-stable SFP state, the spectrum reduces to a single component at the end of the evolution. This requires N to be replaced by an expression for the number of active components, N_a, that varies with evolution time and can be a non-integer, and that applies both as $N_a \to \infty$ and as $N_a \to 1$. An expression with these properties is

$$N_a = \sum_{p=1}^{N} A_p^2 / A_M^2 \tag{A1}$$

The normalisation for W_1 is $N_a^{1/2}$ in order that $|\Psi|$ is unchanged as $N \to \infty$. Regarding W_2, another complication is that some combinations of spectral components have coherent phases, which occurs for values of j, l and m that give $\Phi_{jlmn} = 0$. The summations in (3.15) need to be split into two groups for terms with coherent and non-coherent phases, with different normalisation factors for each group. As shown below, the coherent group itself has two subgroups with different normalisations.

The sum of the coherent terms evolves systematically whereas the sum of the non-coherent terms fluctuates about zero. Because the non-coherent terms depend on Φ_{jlmn}, their prediction requires accurate knowledge of the phases of the components in the perturbation in the initial state. This is often unknown in applications, in which case numerical models can use the summations of the coherent group only. For such cases, the evolution equations (3.23), (3.24) and (3.35) are simplified. The normalisations and resulting evolution equations for the coherent group only are derived below.

Coherent nonlinear terms occur for $\Phi_{jlmn} = 0$, i.e. when $j = m$ or $l = m$, yielding from (3.15)

$$S_{Sn} = 0 \tag{A2}$$

$$S_{Cn} = \sum_{\substack{j+l-m=n \\ 1 \leqslant j,l,m \leqslant N}} A_j A_l A_m \qquad \text{for } j = m \text{ or } l = m \tag{A3}$$

The condition $j + l - m = n$ implies that $l = n$ when $j = m$, and $j = n$ when $l = m$. Thus, (A3) becomes

$$S_{Cn} = A_n \left(\sum_{j=1}^{N} A_j^2 \right) + A_n \left(\sum_{l=1}^{N} A_l^2 \right) - A_n^3 = 2A_n \left(\sum_{j=1}^{N} A_j^2 \right) - A_n^3 \tag{A4}$$

The two summations in the first equation of (A4) are identical. The term that has $j = l = m = n$ is included in both summations, which requires that one of these occurrences is subtracted from the summations, resulting in the $-A_n^3$ term.

The first term in the second equation of (A4) contains the sum of N component combinations and is normalised by the number of active components, N_a. The second term consists of a single component

combination and is normalised by one. Thus, the normalised S_{Cn} (i.e. S_{Cn}/W_2) is determined as

$$\frac{S_{Cn}}{W_2} = \frac{2A_n}{N_a}\left(\sum_{j=1}^{N} A_j^2\right) - \frac{A_n^3}{1} = A_n(2A_M^2 - A_n^2) \tag{A5}$$

The second equation in (A5) follows by substituting (A1) for N_a. Because the normalised variables do not depend on N, the dynamics are unchanged as $N \to \infty$. The ODEs for free evolution using only the coherent nonlinear terms are derived by substituting (A2) and (A5) in (3.13) and (3.14)

$$dA_n/dT = L_{1n}A_n - \mu_r A_n(2A_M^2 - A_n^2) \qquad for\ 1 \leqslant n \leqslant N \tag{A6}$$

$$d\Phi_{nM}/dT = \sigma(L_{2n} - L_{2M} + \mu_i(A_M^2 - A_n^2)) \qquad for\ 1 \leqslant n \leqslant N,\quad n \neq M \tag{A7}$$

$$dK_M/dT = (k_r + K_M)(L_{2M} + \mu_i A_M^2)/C_M \tag{A8}$$

The phase evolution equations (A7) are decoupled from (A6) and (A8).

Appendix B. Galilean invariance of the free evolution equations

Appendix B demonstrates the Galilean invariance of the free evolution equations derived from the CGLe. A Galilean transformation is made from the X, T frame to the $\hat{X}$, $\hat{T}$ frame moving with velocity V in the positive X direction:

$$X = \hat{X} + V\hat{T} \qquad T = \hat{T} \qquad \partial/\partial X = \partial/\partial\hat{X} \qquad \partial/\partial T = -V\partial/\partial\hat{X} + \partial/\partial\hat{T} \tag{B1}$$

The Galilean transformation (B1) is applied to (2.1) to derive the CGLe in the $\hat{X}$, $\hat{T}$ frame

$$\frac{\partial\Psi}{\partial\hat{T}} - V\frac{\partial\Psi}{\partial\hat{X}} = (\gamma_r + i\gamma_i)\Psi + (\alpha_r + i\alpha_i)\frac{\partial^2\Psi}{\partial\hat{X}^2} - (\mu_r - i\mu_i)|\Psi|^2\Psi \tag{B2}$$

The ansatz in the $\hat{X}$, $\hat{T}$ frame is

$$\Psi = (1/W_1)\sum_{n=1}^{N} A_n(\hat{T})\exp[i\sigma\Theta_n(\hat{X},\hat{T})] \qquad \Theta_n = \phi_n(\hat{X},\hat{T}) + \Phi_n(\hat{T})$$
$$\phi_n = K_n(\hat{T})(\hat{X} - X_0 + V\hat{T}) \qquad K_n(\hat{T}) = (n - M)q + K_M(\hat{T}) \qquad \sigma = \pm 1 \tag{B3}$$

Substituting (B3) in the CGLe (B2) gives

$$\sum_{n=1}^{N}[\{dA_n/d\hat{T} - (L_{1n} + i(L_{2n} + \sigma VK_n - \sigma\partial\Theta_n/\partial\hat{T}))A_n\}\exp(i\sigma(\phi_n + \Phi_n))]$$
$$+ (1/W_2)(\mu_r - i\mu_i)\sum_{1\leqslant j,l,m\leqslant N} A_jA_lA_m\exp(i\sigma(\phi_{jlm} + \Phi_{jlm})) = 0 \tag{B4}$$

All parameters are defined in sections 2 and 3, and apply here with $\hat{X}$, $\hat{T}$ as the independent variables. Processing the nonlinear terms similarly to section 3.1.2 transforms (B4) to

$$\sum_{n=1}^{N}[\{(dA_n/d\hat{T} - g_n)/A_n + i(\sigma\partial\Theta_n/\partial\hat{T} - f_n - \sigma VK_n)\}A_n\exp(i\sigma\Theta_n)] = 0 \tag{B5}$$

The following equations, derived from (B3), apply to the relative phases in the $\hat{X}$, $\hat{T}$ frame

$$\Theta_{nM} = (n - M)q(\hat{X} - X_0 + V\hat{T}) + \Phi_{nM} \tag{B6}$$

$$\partial\Theta_{nM}/\partial\hat{T} = d\Phi_{nM}/d\hat{T} + (n - M)qV \tag{B7}$$

The ancillary function, $G_M(\hat{X},\hat{T})$, is introduced in the following expression

$$\sum_{n=1}^{N}[i(\partial G_M/\partial\hat{T} + \sigma VK_M - \sigma\partial\Theta_M/\partial\hat{T})A_n\exp(i\sigma\Theta_n)] \tag{B8}$$

The expression (B8) is added within the summation in (B5) and subtracted as a separate group

$$\sum_{n=1}^{N}\left[\left\{\frac{1}{A_n}\left(\frac{dA_n}{d\hat{T}} - g_n\right) + i\left(\sigma\frac{\partial\Theta_{nM}}{\partial\hat{T}} + \frac{\partial G_M}{\partial\hat{T}} - f_n - \sigma V(K_n - K_M)\right)\right\}A_n\exp(i\sigma\Theta_n)\right]$$
$$- i\left(\frac{\partial G_M}{\partial\hat{T}} + \sigma VK_M - \sigma\frac{\partial\Theta_M}{\partial\hat{T}}\right)\sum_{n=1}^{N} A_n\exp(i\sigma\Theta_n) = 0 \tag{B9}$$

To obtain the general evolution equations, the individual terms in the first summation in (B9) are set to zero. Equation (B12) is used to derive (B11)

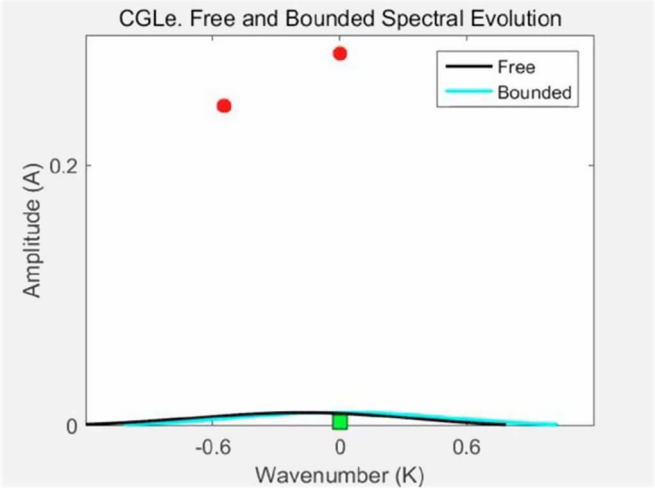

Figure 4. Free and bounded spectral evolution of the CGLe with the same parameter settings. Both spectra grow in amplitude during which the spectral width narrows. The final states are finite-amplitude plane waves. For free evolution, the spectrum as a whole shifts to lower wavenumbers, whereas for bounded evolution the spectral peak wavenumber remains unchanged.

$$dA_n/d\hat{T} = g_n \qquad for\ 1 \leqslant n \leqslant N \tag{B10}$$

$$\partial\Theta_{nM}/\partial\hat{T} = \sigma(f_n - f_M) + V(K_n - K_M) \qquad for\ 1 \leqslant n \leqslant N,\quad n \neq M \tag{B11}$$

$$\partial G_M/\partial\hat{T} = f_M \tag{B12}$$

From (B7), (B11) and (B3)

$$d\Phi_{nM}/d\hat{T} = \sigma(f_n - f_M) \qquad for\ 1 \leqslant n \leqslant N,\quad n \neq M \tag{B13}$$

The last term in (B9) is required to be equal to zero, giving $\partial G_M/\partial\hat{T} = -\sigma V K_M + \sigma\partial\Theta_M/\partial\hat{T}$. Using (B3), this requirement is expressed as

$$\partial G_M/\partial\hat{T} = \sigma(\hat{X} - X_0 + V\hat{T})dK_M/d\hat{T} + \sigma d\Phi_M/d\hat{T} \tag{B14}$$

The particular solution for free evolution is derived by returning to the $X,\ T$ frame, in order to separate distance and time variables in the expressions for phase, i.e. the form $K_M(T)(X - X_0)$ rather than $K_M(\hat{T})(\hat{X} - X_0 + V\hat{T})$ is required. The analysis continues in this frame until F_M is derived as (3.33) and $\partial F_M/\partial T$ as (3.34). G_M is now defined such that

$$\partial G_M/\partial\hat{T} = \partial F_M/\partial T \tag{B15}$$

Equation (3.34) is transformed back to the $\hat{X},\ \hat{T}$ frame by (B15) and (B1)

$$\partial G_M/\partial\hat{T} = [C_M/(k_r + K_M(\hat{T}))]dK_M/d\hat{T} \tag{B16}$$

Comparing (B16) with the validity condition (B14) shows that

$$d\Phi_M/d\hat{T} = 0 \tag{B17}$$

$$\sigma(\hat{X} - X_0 + V\hat{T}) = C_M/(k_r + K_M) \tag{B18}$$

The evolution equation for K_M is obtained from (B16) and (B12)

$$dK_M/d\hat{T} = (k_r + K_M)f_M/C_M \tag{B19}$$

The dispersion equation for a general component n is derived using (B3), (B13), (B17), (B18) and (B19)

$$\Omega_n = -\partial\Theta_n/\partial\hat{T} = -\sigma f_n - VK_n \tag{B20}$$

The outcome is that the evolution equations (B10), (B13) and (B19) are unchanged in the $\hat{X},\ \hat{T}$ frame compared with (3.23), (3.24) and (3.35) in the $X,\ T$ frame. Wave frequencies undergo a Doppler shift by $-VK_n$ in (B20) compared with (3.41) in the $X,\ T$ frame.

Appendix C. Video of free and bounded evolving solutions of the CGLe

Appendix C presents a video of free and bounded evolving solutions of the CGLe (figure 4). It is available in the online html version of the paper only. The runtime is 76 s.

The video shows simultaneous free (black line) and bounded (light blue line) evolution of wave spectra in a wavenumber-amplitude plot. These lines are identified in the legend. Both spectra have the same equation constants shown in the figure 2 caption. They evolve from the same initial low-amplitude spectrum (centred on the green square) towards final sideband-stable SFP states (red circles).

The equations for free evolution are (A6) and (A8), which have only coherent nonlinear terms. For bounded evolution, (A8) is replaced by $dK_M/dT = 0$. The characteristic value for free evolution is $C_M = -\pi$. The numerical solution uses a fourth-order Runge–Kutta timestepping scheme. The spectra contain 3001 wavenumber components, the computational timestep is 0.00277 and the evolution time is 3800 timesteps.

ORCID iDs

Howard N Southgate https://orcid.org/0000-0003-2065-5197

References

[1] Aranson I S and Kramer L 2002 The world of the complex Ginzburg–Landau equation *Rev. Mod. Phys.* **74** 99–144
[2] Liu W-M and Kengne E 2019 *Schrödinger Equations in Nonlinear Systems* (Pub. Springer Nature)
[3] Debnath L 2012 *Nonlinear Partial Differential Equations for Scientists and Engineers* third edition (Pub. Birkhäuser)
[4] Garcia-Morales V and Krischer K 2012 The complex Ginzburg–Landau equation: an introduction *Contemp. Phys.* **53** 79–95
[5] Stuart J T and DiPrima R C 1978 The Eckhaus and Benjamin-Feir resonance mechanisms *Proc. R. Soc.* A **362** 27–41
[6] Doelman A 1991 Finite dimensional models of the Ginzburg–Landau equation *Nonlinearity* **4** 231–50
[7] Keefe L R 1985 Dynamics of perturbed wavetrain solutions to the Ginzburg–Landau equation *Stud. Appl. Maths* **73** 91–153
[8] Moon H T, Huerre P and Redekopp L G 1983 Transitions to chaos in the Ginzburg–Landau equation *Physica* D **7** 135–50
[9] Nana L, Ezersky A B and Mutabazi I 2009 Secondary structures in a one-dimensional complex Ginzburg–Landau equation with homogeneous boundary conditions *Proc. R. Soc.* A **465** 2251–65
[10] Cross M C and Hohenberg P C 1993 Pattern formation outside of equilibrium *Rev. Mod. Phys.* **65** 851–1112
[11] Bekki N and Nozaki K 1985 Formations of spatial patterns and holes in the generalized Ginzburg–Landau equation *Phys. Lett.* **110A** 133–5
[12] Van Saarloos W and Hohenberg P C 1992 Fronts, pulses, sources and sinks in generalized complex Ginzburg–Landau equations *Physica* D **56** 303–67
[13] Lega J 2001 Traveling hole solutions of the complex Ginzburg–Landau equation: a review *Physica* D **152** 269–87
[14] Chomaz J-M 2005 Global instabilities in spatially developing flows: non-normality and nonlinearity *Ann. Rev. Fluid Mech.* **37** 357–92
[15] Djazet A, Fewo S I, Tabi C B and Kofané T C 2021 Dynamics of moving cavity solitons in two-level laser system from symmetric gaussian input: vectorial cubic-quintic complex Ginzburg–Landau equation *Appl. Phys.* B **127** 151
[16] Gil L 1993 Vector order parameter for an unpolarised laser and its vectorial topological defects *Phys. Rev. Lett.* **70** 162
[17] Schielen R, Doelman A and De Swart H E 1993 On the nonlinear dynamics of free bars in straight channels *J. Fluid Mech.* **252** 325–56
[18] Fujita Y and Muramoto Y 1985 Studies on the process of development of alternate bars *Bulletin Disaster Prevention Research Inst., Kyoto Univ.* **35** 55–86 (https://cir.nii.ac.jp/crid/1050001202065160448)
[19] Garcia M and Niño Y 1993 Dynamics of sediment bars in straight and meandering channels: experiments on the resonance phenomenon *J. Hydr. Res.* **31** 739–61
[20] Lanzoni S 2000 Experiments on bar formation in a straight flume 1. Uniform sediment *Water Resour. Res.* **36** 3337–49
[21] Crosato A, Mosselman E, Desta F B and Uijttewaal W S J 2011 Experimental and numerical evidence for intrinsic nonmigrating bars in alluvial channels *Water Resour. Res.* **47** W03511
[22] Crosato A, Desta F B, Cornelisse J, Schuurman F and Uijttewaal W S J 2012 Experimental and numerical findings on the long-term evolution of migrating alternate bars in alluvial channels *Water Resour. Res.* **48** W06524
[23] Duró G, Crosato A and Tassi P 2016 Numerical study on river bar response to spatial variations of channel width *Adv. Water Res.* **93** 21–38
[24] Choi B, Jeong D and Choi M Y 2016 General method to solve the heat equation *Physica* A **444** 530–7
[25] Gilboa G, Sochen N and Zeevi Y Y 2004 Image enhancement and denoising by complex diffusion processes *IEEE Trans. Pattern Anal. Mach. Intell.* **26** 1020–36
[26] Akulenko L D and Nesterov S V 2008 Elastic properties of a fluid-saturated granular medium, *Mech. Solids* **43** 1–12
[27] Møller P C F and Bonn D 2007 The shear modulus of wet granular matter *EPL* **80** 38002